NASA CONTRACTOR REPORT

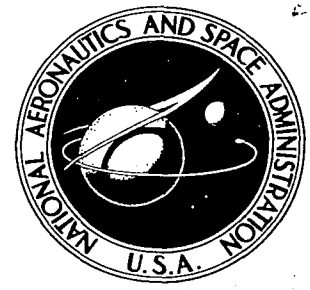

NASA CR-397

PHOTOELECTRIC DETECTION OF WEAK SPECTRUM LINES

by R. T. Schneider and R. O. Whitaker

Prepared under Contract No. NASw-922 *by*
GENERAL MOTORS
Indianapolis, Ind.
for

NATIONAL AERONAUTICS AND SPACE ADMINISTRATION • WASHINGTON, D. C. • MARCH 1966

NASA CR-397

PHOTOELECTRIC DETECTION OF WEAK SPECTRUM LINES

By R. T. Schneider and R. O. Whitaker

Prepared under Contract No. NASw-922 by
GENERAL MOTORS
Indianapolis, Ind.

for

NATIONAL AERONAUTICS AND SPACE ADMINISTRATION

For sale by the Clearinghouse for Federal Scientific and Technical Information
Springfield, Virginia 22151 – Price $2.00

PHOTOELECTRIC DETECTION OF WEAK SPECTRUM LINES

By R. T. Schneider and R. O. Whitaker
Allison Division of General Motors

SUMMARY

The application of integrating electronic devices to optical spectroscopy is demonstrated. It is shown that weak spectrum lines can be detected, even if the photomultiplier output, developed in response to the lines, is many orders of magnitude below the noise level. It is also demonstrated that the line shape can be determined. The electronic devices used are discussed and their performance is compared.

INTRODUCTION

The spectrum in the focal plane of a spectrograph can be detected either photographically or photoelectrically. The photographic detection results in a two-dimensional picture; one dimension (usually lateral position) indicates the wavelength while the other dimension (length of the spectrum line) indicates a geometric dimension of the light source—e.g., diameter of an arc. The degree of blackening of the photographic emulsion indicates intensity of the light source.

Photoelectric detection gives a trace indicating intensity versus wavelength. It cannot indicate a geometric dimension of the light source. This disadvantage can sometimes be overcome by taking readings from different regions of the light source. The photoelectric sensor, usually a photomultiplier tube, does not integrate over time. Therefore, if the sensitivity of

photographic detection is compared with the sensitivity of photoelectric detection, photoelectric detection is superior for short-time application; photographic detection is superior for long exposure times.

Experiments reported here show that auxiliary electronic equipment will permit photoelectric detection to be used in a time-integrating manner. Results indicate that for applications where long exposure times are possible, the sensitivity of photoelectric detection becomes equal to (or even better than) the sensitivity of photographic detection.

A second advantage of photoelectric recording lies in the fact that the electrical output of the photocathode bears a linear relationship to light falling thereon. Density on a photographic plate is logarithmically related to light input.

A third advantage is that no processing (comparable to development of a photographic plate) of the electrical signal is required. Consequently, no errors can result therefrom.

The output of a photomultiplier is a convenient electrical signal which can be amplified conveniently. This permits extremely weak signals to be detected. The limitation on amplification is imposed by the noise of the photocathode and related electronic components. Therefore, a time-integrating circuit for the photomultiplier to enable it to detect extremely weak signals would be advantageous only if this circuit were able to suppress the noise.

This report discusses the application of two such noise suppression systems to optical spectroscopy. An optical arrangement is first described. A few simple tests are discussed which show that it is possible to detect weak lines and to show their true shape.

Methods for detecting electrical signals buried in noise have been developed recently for space communication. These methods have been applied to the

study of brain waves and to the study of nuclear magnetic resonance.* The object of the present report is to discuss their applicability to spectroscopy.

APPLICATION OF INTEGRATING COMPONENTS FOR DETECTION OF WEAK LINES

Photoelectric Detection of Weak Lines

The optical setup used in the present tests is indicated in Figure 1. The entrance slit was illuminated by a W-ribbon lamp. The grating was placed in zero-order position and adjusted so that the image of the entrance slit lay on the exit slit. The rotating prism swept the image of the entrance slit across the exit slit. The resulting signal developed by the photomultiplier assumes a triangular shape, provided both slits are adjusted to the same width. The intensity of the lamp was adjusted to render the signal easily visible, permitting the shape of the signal to be observed. The intensity was then reduced until the signal disappeared in the electronic noise of the photomultiplier.

For other tests the W-ribbon lamp was replaced by a mercury lamp or an argon arc. During these tests, the grating was put in first- or second-order position. The shape of the signal was then determined by the line profile. The output of the photomultiplier was amplified and displayed on an oscilloscope. The oscilloscope was triggered by a unit (not shown in Figure 1) mechanically connected to the rotating prism. As a result, the signal always appeared at the same position on the oscilloscope screen.

Figure 2 is an oscilloscope picture of the signal coming from the W-ribbon lamp (grating in zero-order position).

---

*M. P. Klein, and G. W. Barton, "Enhancement of Signal-to-Noise Ratio by Continuous Averaging: Application to Magnetic Resonance," The Review of Scientific Instruments, Vol 34, No. 7 (July 1963).

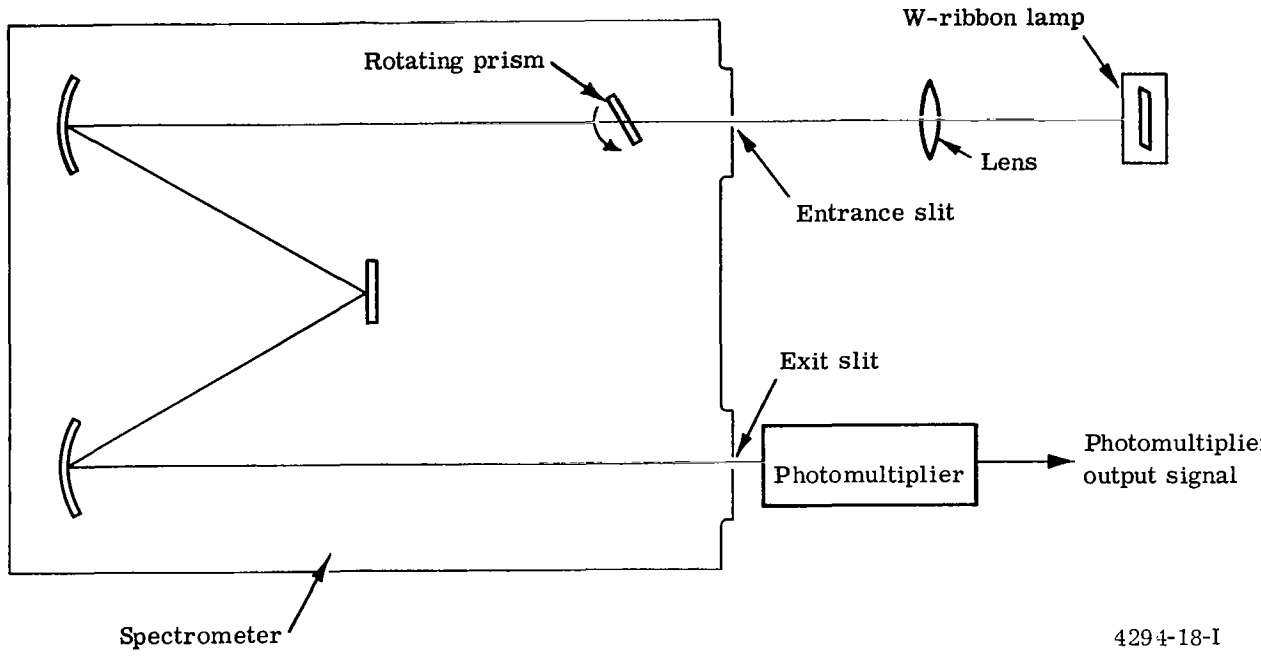

Figure 1. Optical test setup used to detect extremely weak light signals.

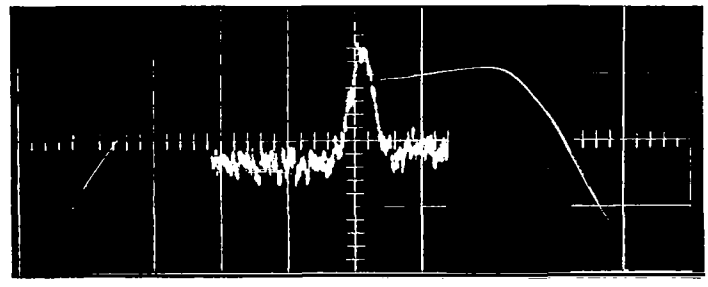

Figure 2. Intensity profile of a W-ribbon taken with a photomultiplier.

Figure 3 shows the signal obtained after the intensity of the lamp was reduced so that the triangular (real) signal disappeared amid the random noise. The oscilloscope trace was exposed long enough to record many sweeps. It would have been possible, however, to photograph only a single sweep. Even if this had been done, no real signal would have been visible.

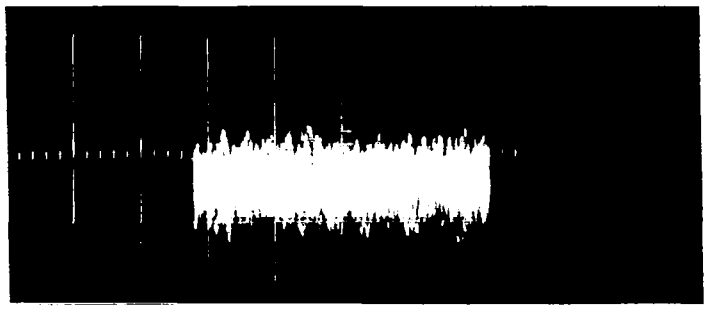

Figure 3. Intensity profile of a W-ribbon with the signal buried in noise.

The mixture of random noise and the real signal, as shown in Figure 3, was integrated electronically. A detailed discussion of the electronic integration techniques is given in the subsection titled Electronic Component for Integrating.

Figure 4 indicates the result of the integration. Parts a, b, c, and d correspond to different exposure times (different integration times). As can be seen, the real signal has resumed the triangular shape of the original signal. Comparison showed that it is identical. The original signal, hidden in Figure 3 and recovered in Figure 4, was extremely weak. The intensity of the W-ribbon lamp which emits this signal was turned down so far that the radiation of the W-ribbon could not be detected with the eye. In the case of Figure 4, the entrance slit of the spectrometer was only 2 mm high and 5 μ wide. The photomultiplier used was a Type 7102.

For the next test, the W-ribbon lamp was replaced by an argon arc. The Type 7102 photomultiplier was replaced by a 1P28. The grating was set in first-order position. Argon lines 4333.56 and 4335.35Å were swept across the exit slit by the rotating prism. The intensity of the argon arc was reduced by a variable aperture until the lines disappeared amid the electronic noise. A photograph of the resultant oscilloscope trace is shown in Figure 5. For this trace, only a single sweep was photographed. A multiple-sweep would

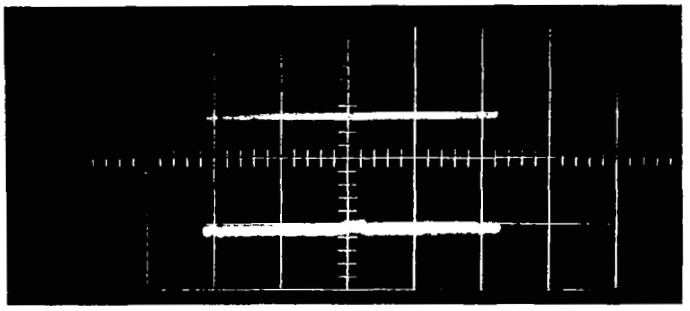

a. 5 sec

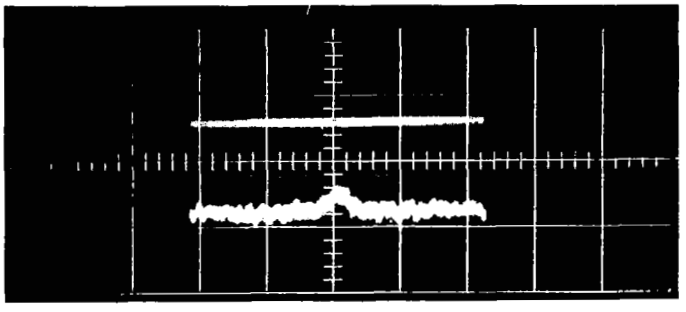

b. 10 sec

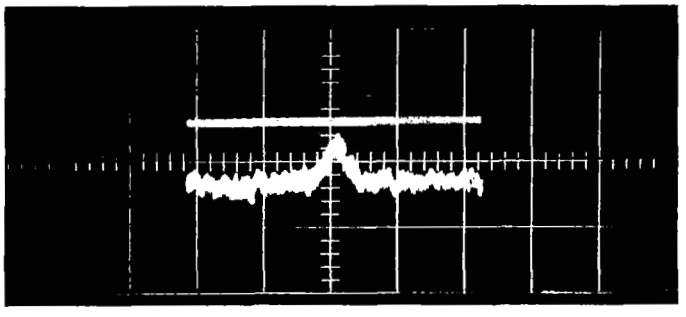

c. 15 sec

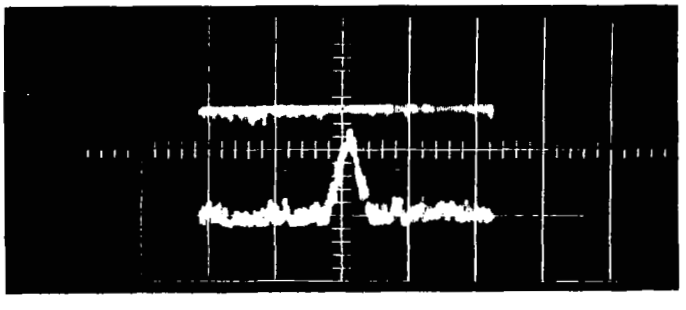

d. 20 sec

Figure 4. Signal buried in noise at various integration times.

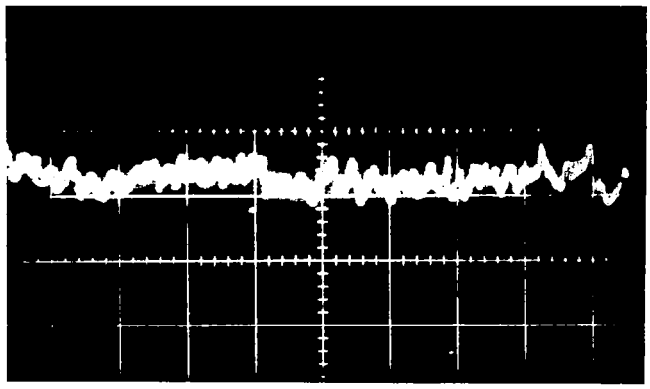

Figure 5. Single sweep oscilloscope trace of a 1P28 photomultiplier output. Signal buried in noise (argon lines 4333.56 and 4335.35 Å).

have resulted in a 1-cm wide band similar to that shown in Figure 3. Again, the mixture of random noise and real signal was integrated and the real signal recovered. The result is shown in Figure 6.

Figure 6 demonstrates that integration techniques are applicable to spectroscopy. The electrical signal produced by the line radiation was so weak relative to the photocathode noise that the conventional photoelectric detection technique would have been completely unable to reveal the lines. This is clearly shown in Figure 5. The integration techniques not only reveal the lines present but also indicate relative intensities of the lines.

It has been demonstrated that integration techniques permit photoelectric detection of weak lines which otherwise could not be detected photoelectrically. However, it has not been shown that they could not be detected photographically. This subject is discussed in a later subsection.

One important advantage of modified photoelectric detection can be pointed out at once. Assume that, in addition to the weak line radiation, a strong continuous radiation is present. Due to the logarithmic sensitivity of the photographic plate, it would be very difficult to detect the weak lines photographically. Even if the weak lines are strong enough to be detected by themselves,

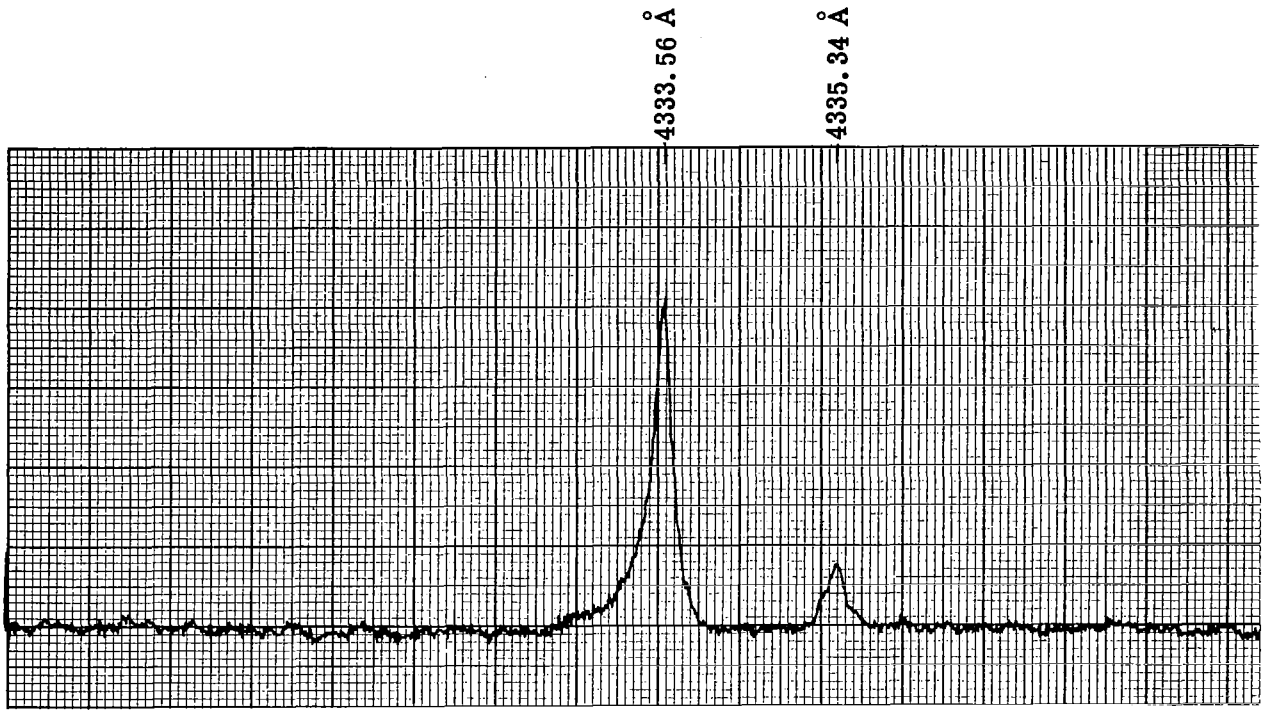

Figure 6. Signal of Figure 5 after integration (argon lines 4333.56 and 4335.35 Å).

they might not be detected when the continuous radiation is also present. In such case, photoelectric setup described has a clear advantage. Due to the "chopping" action of the rotating prism, the continuous radiation can be filtered out as a d-c component at the very first amplification stage. The incoming continuous radiation, however, may saturate the photomultiplier as well as the photographic plate. The intensity of the incoming radiation, therefore, must be reduced in both cases by an aperture or filter. This also decreases the intensity of the already weak lines. To recover the weak lines in the case of photoelectric recording, the integration (in the case of the photographic recording, the exposure time) must be increased. However, increase of exposure time in the photographic case does not help, since the continuum is increased also. In the photoelectric case the continuous radiation, being a d-c component, can be eliminated. Therefore, it is only a matter of a sufficiently large integration time to bring out the lines.

Detection of the True Line Shape

The mere detection of the fact that a certain line is present is very valuable. However, it is also most desirable to detect the shape of this line. This is mandatory in some applications, such as measurement of electron density with Stark broadening. Here it is very important to be able to detect the true profile of weak lines since it is generally the weak lines which show appreciable broadening.

To investigate whether the line shape is changed during the integration process, the following test was made. A line doublet with lines 0.4Å apart was selected (mercury lines at 3662.87 and 3663.27Å). The intensity of the lines was sufficient so that the lines could be observed easily. The optical arrangement was the same as shown in Figure 1, except that the W-ribbon lamp was replaced by a Hg lamp and the grating was in second-order position. Since the spectrograph could not completely resolve the line pair, the resultant line had a very distinctive shape. The intensity was then reduced until the signal height was of the same order of magnitude as the noise level. The oscilloscope trace of the line pair under these conditions is shown in Figure 7. This signal was integrated and displayed on an x-y recorder. The result is shown in Figure 8. The trace obtained is (within the error of measurement) identical with the trace obtained before the intensity was reduced.

Comparison with Photographic Detection

This section discusses whether or not the lines detected with integration could be detected photographically under identical circumstances. The setup shown in Figure 1 was used. The photomultiplier was replaced by a camera attachment. The rotating prism was not required; however, it was used because an identical optical setup was desired as a basis for comparison. Figure 9 shows the results of the sensitivity test using photomultipliers Types 7201 and 1P28.

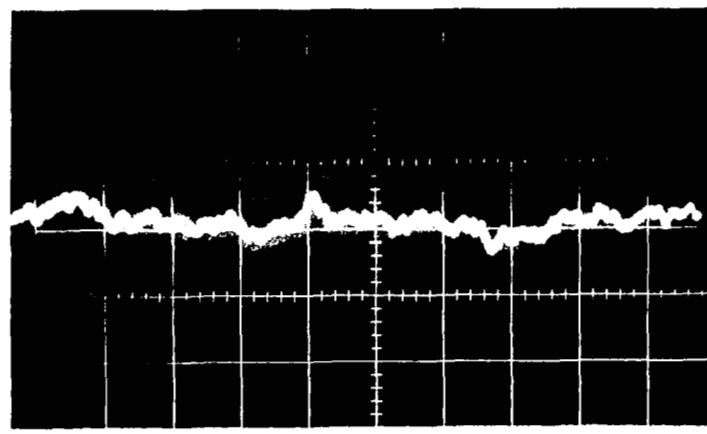

Figure 7. Signal output of photomultiplier.

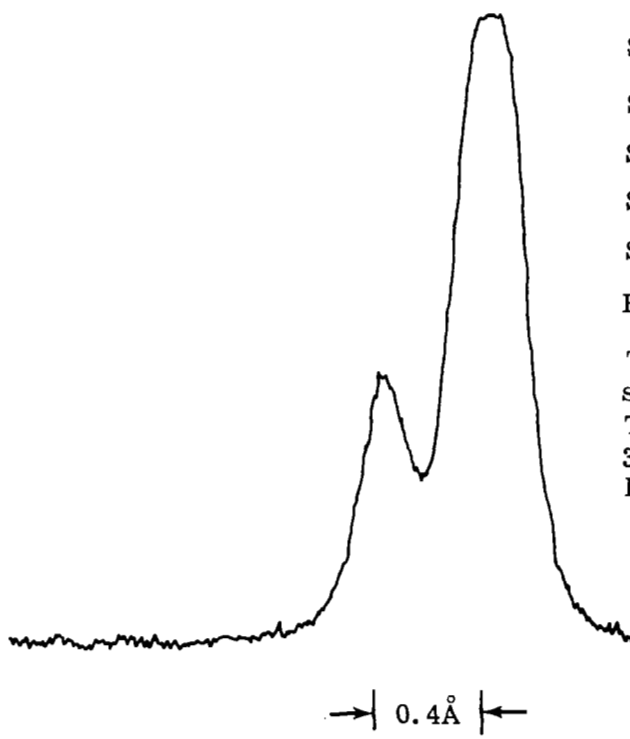

Mercury lines—3662.87 (50)
3663.27 (500)

Spex 0.75 meter

Spectrometer

Slit width—10 microns

Slit height—2 mm

Scanning time—0.038 sec for 1024 points

Excitation—low pressure mercury arc

The stronger line (3663.27 Å) is electronically saturated and appears at a reduced height. This is done intentionally, since otherwise the 3662.87 Å line would be only a small pip on the larger one.

Figure 8. Signal of Figure 7 after integration.

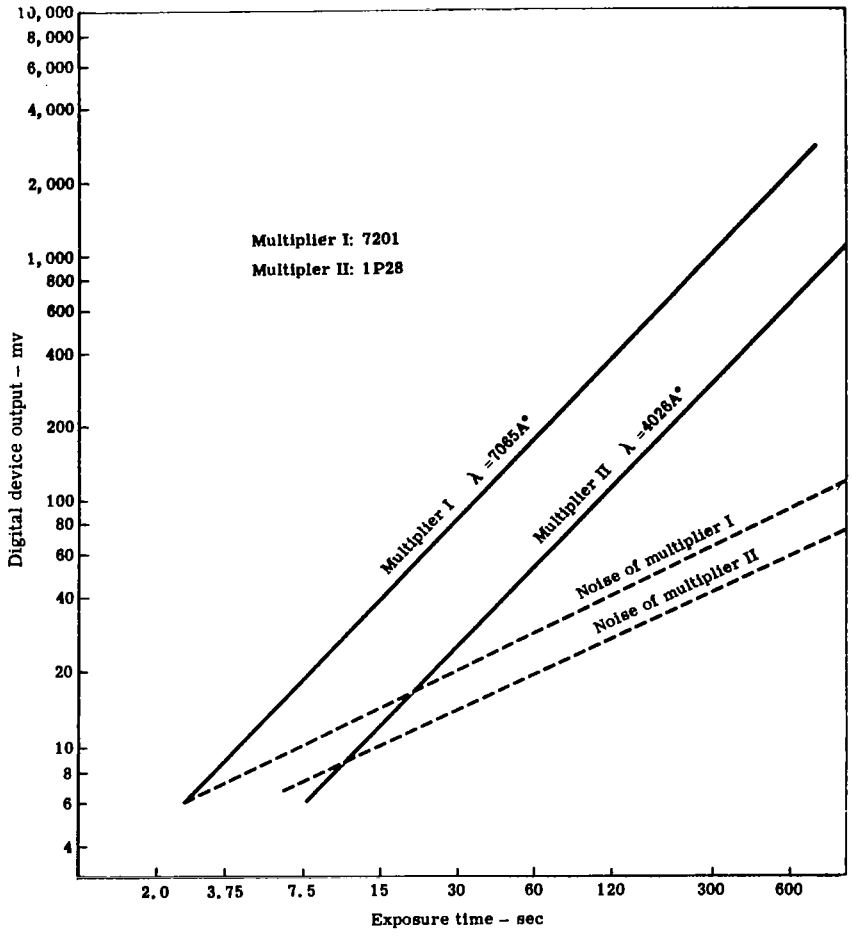

Figure 9. Multiplier output response curves.

Signals I and II emerge from the noise after approximately 3 and 12 sec exposure time and rise in proportion to the exposure time. The noise rises as the square root of time, so that after approximately 120 sec, signal I is approximately ten times stronger than the noise. At 300 sec, signal I is 17 times stronger, etc.

Figure 10 shows the results of the sensitivity test using photoplates (Kodak NI, Developer D19, 5 min developing time). The sensitivity curves in Figure 10 are straight lines because W-values were used as ordinates. The W-value of the Seidel transformation is defined by:

$$W = \log \frac{A_o}{A} - 1$$

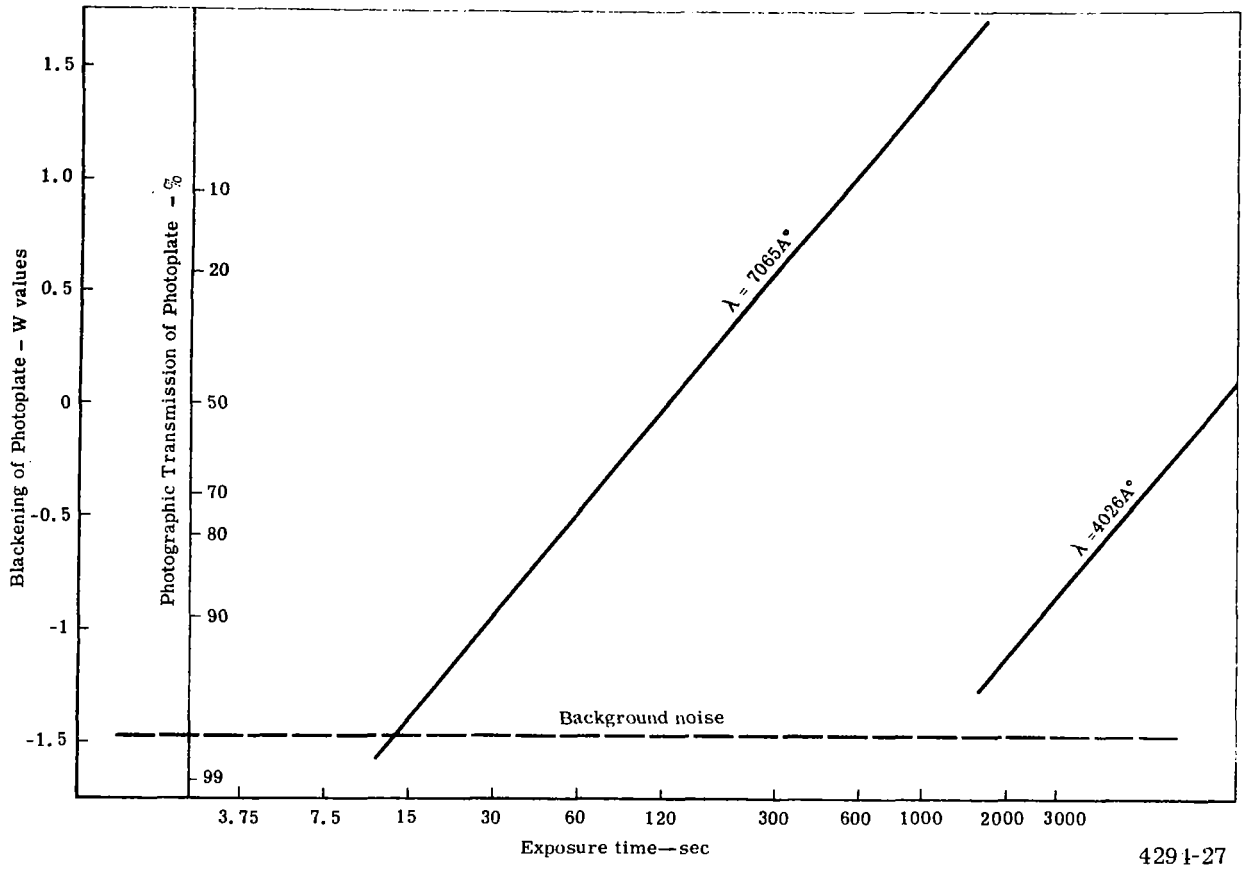

Figure 10. W-values versus exposure times for two wavelengths of light.

where A_o is the photometer reading of the clear photoplate and A is the photometer reading of the blackened photoplate. The signal on the photoplate becomes detectable for λ = 7065Å after 15 sec exposure time. This compares with 3 sec integration time for the photoelectric detection. In the case of λ = 4026Å, the comparison is even more in favor for the photoelectric detection with 12 versus 1000 sec. However, the emulsion used, NI, is not the most sensitive available for this wavelength. Therefore, this ratio could be improved.

It is concluded that photoelectric detection is at least as sensitive as photographic detection.

ELECTRONIC COMPONENT FOR INTEGRATING

Digital Method

A typical experimental setup is shown in Figure 11. The signal appearing at "a" is noise plus the real signal. The real signal is cyclic, having a fundamental frequency equal to the scanning rate. The highest frequency component may be determined by Fourier analysis if the profile of the signal is known. It is necessary that the amplifier pass ac only. Its bandpass should be flat between the fundamental and the high frequency limit—the amplifier need pass nothing outside this band. The effective value of the noise in the output of the amplifier can be reduced by installing filters which limit the bandpass to that required by the real signal. The signal at "b" should have a peak value slightly less than one volt. A higher value will overload the input circuits to the digital device.* A lower value will increase the integration time unnecessarily. During test, this signal should be monitored on an oscilloscope. The signal consists of the real signal plus noise components lying in the bandpass of the amplifier.

The digital device is designed to effectively discover repetitive signals buried in noise. There are two requirements for the input to this device.

- The real signal must be repetitive.
- A triggering signal must be available. The real signal must be delayed with respect to the triggering signal by the same time period each cycle. However, triggering signals need not be evenly spaced in time.

In the present case, the triggering signal was taken from a silicon cell struck by light reflected from the rotating prism.

---

*The name "digital device" as used in this report refers to the Enhancetron, a statistical instrument produced by the Nuclear Data Corporation.

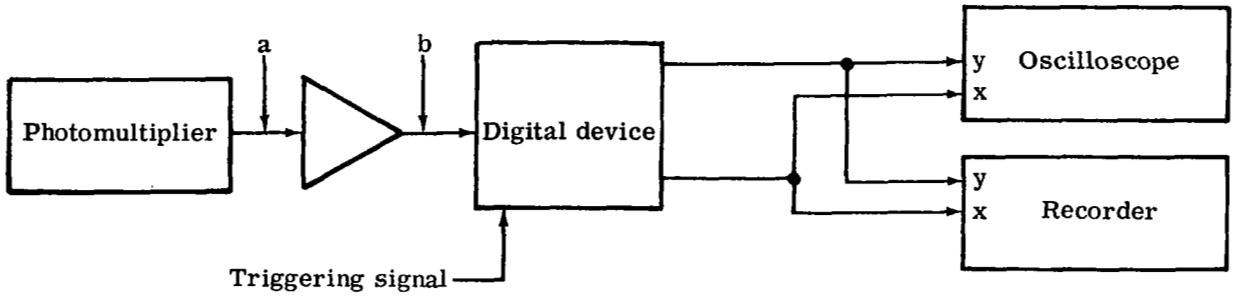

Figure 11. Digital device setup.

Two oscilloscopes are necessary—one to monitor the signal input to the digital device, the other to monitor the signal being built up in the memory of the digital device. Alternatively, one oscilloscope may be switched between the two observation points.

A recorder is convenient for giving a permanent record. However, photographs from the second oscilloscope are adequate.

The operational procedure is as follows.

- Adjust amplifier gain until input to the digital device shows peaks just less than one volt.
- Start the digital device.
- Watch the signal build up on the second oscilloscope. When the signal-to-noise ratio becomes adequate, stop the digital device.
- Record the contents of the digital device memory.

GATED FILTER METHOD

A setup diagram for the gated filter is shown in Figure 12.

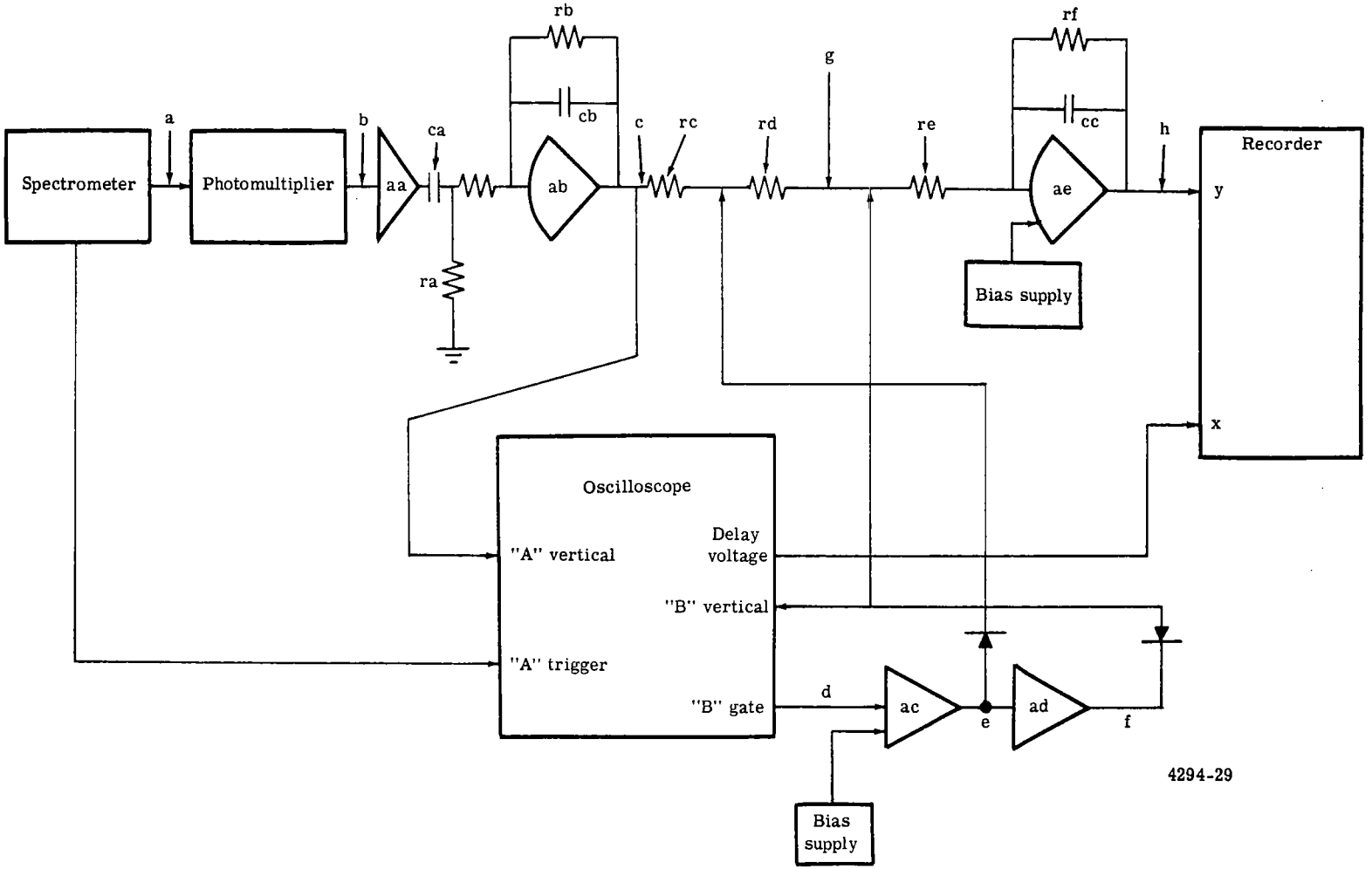

Figure 12. Gated filter setup.

The output of the spectrometer may be represented by signal "a" as indicated in Figure 13. The spectrum has one prominent line at phase "m" and a weak line at phase "n."

The output of the photomultiplier may be represented by signal "b" of Figure 13. Noise generated by the photomultiplier obscures the shape of the signal at phase "m." The weak signal at "n" is no longer detectable.

Amplifier "aa" raises the millivolt signal obtained from the photomultiplier to about 35 v. The amplifier should have a bandpass flat from the scanning rate frequency to the highest significant harmonic of the signals sought.

Operational amplifier "ab" (from an analog computer facility) facilitates the trial of filters. Capacitor "ca" and resistor "ra" permit the low frequency cutoff to be varied. Capacitor "cb" permits the high frequency cutoff to be varied. Output of amplifier "ab" is given by trace "c" of Figure 13. High frequency components are absent.

The oscilloscope is a dual beam unit with separate sweep generators. A facility is included which permits the B trace (Figure 12) to be delayed with respect to the A trace. The A trace is triggered by the rotating prism. Sweep time is adjusted to show the spectrum of interest. The B sweep is delayed and given a higher sweep rate. The resultant B gate signal is indicated by trace "d" of Figure 13. By varying the delay, the initial point of the gate may be moved along the abscissa. By varying the B sweep rate, the width of the gate may be varied.

Operational amplifiers "ac" and "ad" give low output impedance gate signals both positive and negative. Gate signal "e" is given in Figure 13. Gate "f" is the same as "d."

The gate is adapted to permit the input signal "c" to pass only while the B gate is "On." Trace "g" of Figure 13 illustrates the gated signal corresponding to gate "d." Resistor "rc" prevents overload of amplifier "ab." Resistor

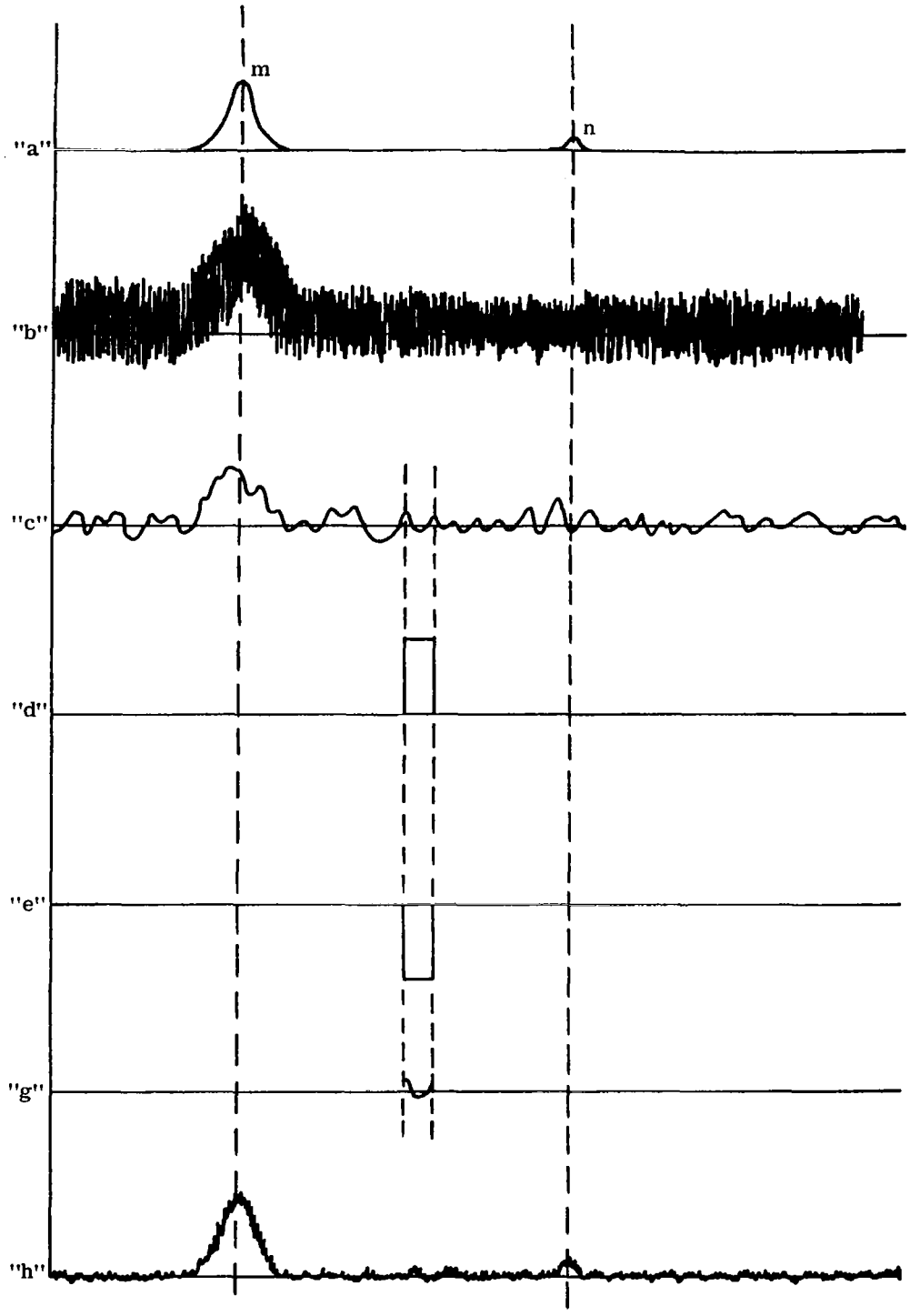

Figure 13. Gated filter system signals.

"rd" prevents large circulating currents through the diodes which might result from small unbalance in amplifiers "ac" and "ad." The bias supply feeding to amplifier "ac" serves to adjust the balance.

The circuit of operational amplifier "ae" is essentially a low-pass filter. The time constant of the "rf-cc" combination is generally several seconds. If the sweep rate is about ten per second, the filter provides effective integration. Resistors "re" and "rf" should be chosen to give high amplification. A bias supply is adjusted to hold average amplifier output to zero. Output "h" is an undulating d-c signal roughly proportional to the real signal present in the gated portion of the system input signal.

The oscilloscope circuit developing the delay provides a voltage proportional to the delay. This voltage is taken from the oscilloscope and fed to the abscissa of the recorder.

In searching for weak signals buried in noise, the delay potentiometer of the oscilloscope is varied, causing the gate to move along the traces of Figure 13. The recorder indicates the recovered signal. Trace "h" indicates what could be expected from input "b."

Digital Device Results

In the current tests, the photomultiplier of Figure 11 was replaced by the system of Figure 14. A noise generator provided a noise signal. A sweep generator feeding a function generator provided a simulated real signal. The two signals were mixed into the amplifier. The potentiometers permitted the proportion to be varied. A synchronization pulse was taken from the sweep generator for triggering of the oscilloscope.

The photographs of Figure 15 indicate system performance. They are, in order:

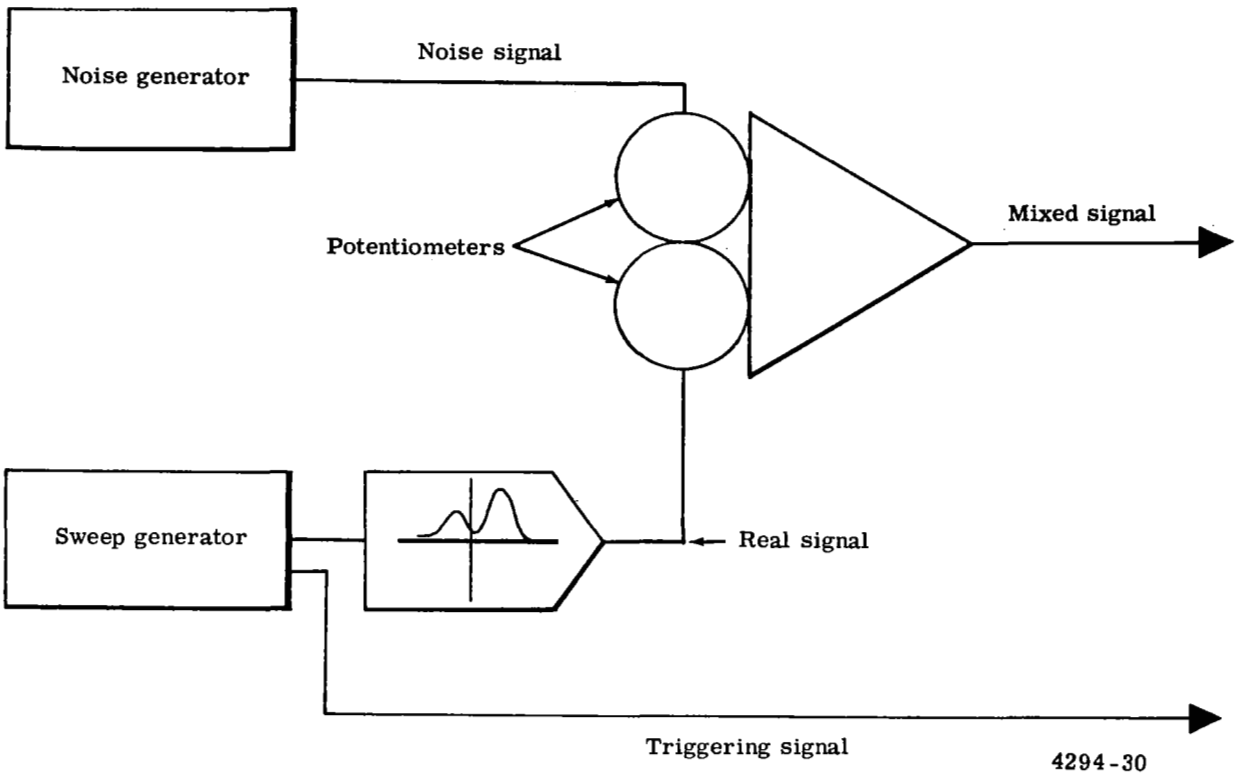

Figure 14. Photomultiplier signal simulator.

26-1 The real signal without noise (The signal is the line in the lowest band. A slight rise is visible 0.5 cm to the left of center. A larger rise is shown 1.5 cm to the right of center.)

26-2 The real signal with the vertical scale expanded by ten

26-3 The noise signal by itself

26-4 Noise plus real signal

26-5 About ten overlapping traces of noise plus real signal (Note that the real signal is not even slightly visible.)

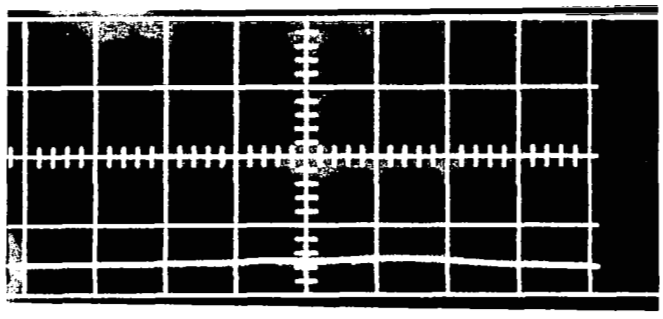

Trace 26-1

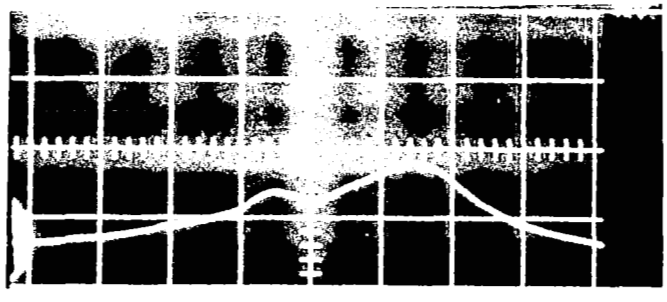

Trace 26-2

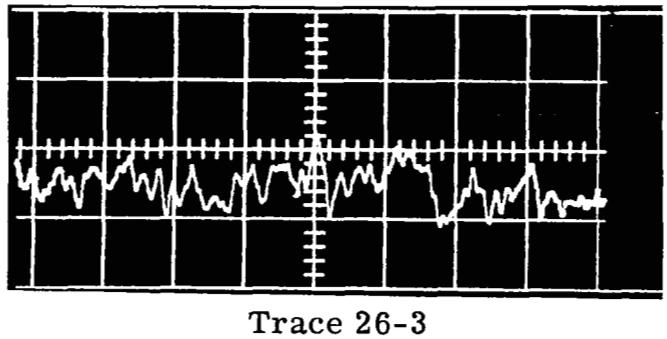

Trace 26-3

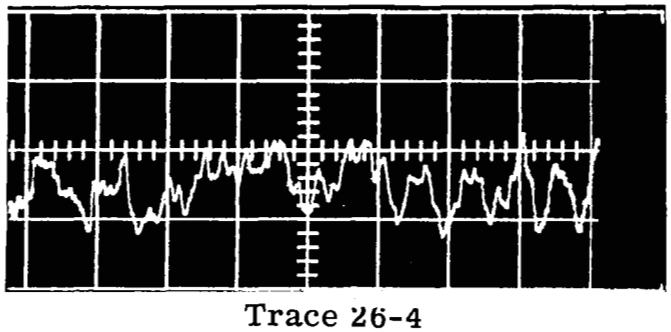

Trace 26-4

Figure 15. Digital device system performance.

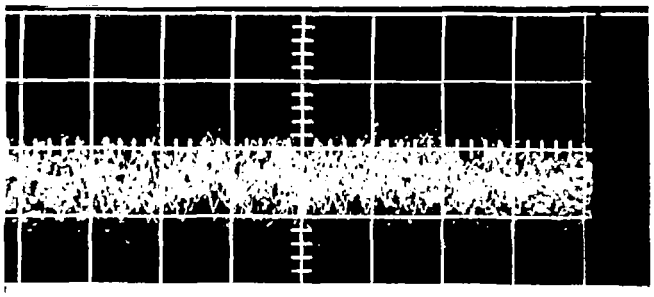

Trace 26-5

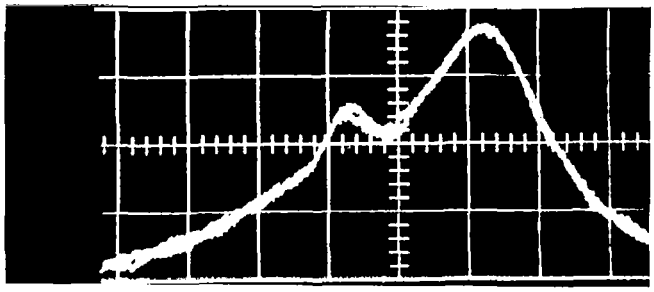

Trace 26-6

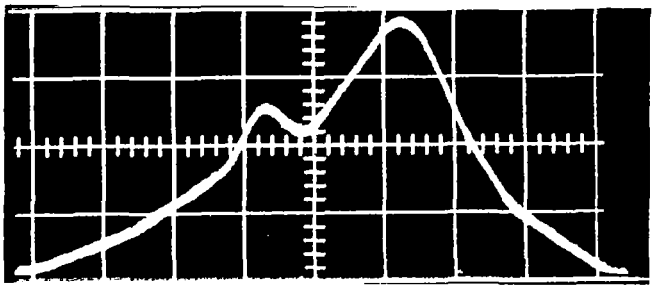

Trace 26-10

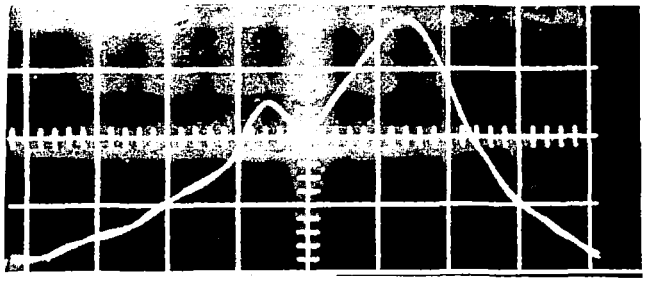

Trace 26-11

Figure 15. Digital device system performance.

26-6 Trace developed by the digital device after 75 sec of integration. (The clearly evident double trace appearing 0.5 cm to left of center and elsewhere will be discussed later.)

26-10 Trace after 600 sec—virtually a perfect replica of the real signal of photo 26-2

In this test the real signal was small and was invisible amid the noise. Actually, it could be reduced further by several orders of magnitude and still be detectable with the digital device. Trace 26-6 indicates the maximum noise amplitude to be about 5% of the maximum real signal. Hence, 75 sec integration time should give a unity signal-to-noise ratio for a signal only 5% as great as that used to obtain trace 26-6. For an integration time of 600 sec, the real signal could be reduced still further.

The limit of detectability for the digital device is reached when noise alone overloads the memory locations. Trace 26-10 indicates noise to be about 5% of full scale. Noise signals build up as the square root of time. Consequently, noise overload would not occur until after 240,000 sec—about three days. Real signals build up in direct proportion to integration time. Consequently, the minimum detectable real signal is 4000 times smaller than that used in the present tests. The digital device may be used to detect signals for which the signal-to-noise ratio is about 0.00025.

Reference is made to the double trace of photo 26-6 (Figure 15). It was found that the output of the function generator carried a 60-cps hum voltage of comparable magnitude. Photo 26-11 (Figure 15) shows two traces of the function generator output—the sweep rate was 10 cps. Such hum voltages constitute a noise input if they are not synchronized with the sweep and a real signal if they are synchronized with the sweep. In using the digital device, care must be exercised to eliminate such repetitive signals. If they cannot be eliminated, care should be taken to ensure that they are not synchronized with the sweep.

The similarity in appearance of the hum signal of photo 26-11 and output trace 26-6 indicates that some internal characteristic of the digital device permitted the apparent modulation. It is significant that the double trace disappeared as integration time became longer. It is possible that noise alone accounts for the double trace.

In searching for weak signals, the optical spectrum width observed should be reduced to a minimum. The observed spectrum should resemble that of photo 26-2 rather than trace "a" of Figure 13. The real signal of trace "a" will contain significant harmonics far higher than those contained in the real signal of photo 26-2. Consequently, a more restricted system band width may be employed for signals which fill the greater portion of the observed optical spectrum. More of the noise can be removed by conventional filters. It follows that rotating prisms are not as satisfactory for searching for very weak signals as are vibrating mirrors. The amplitude of vibration of the vibrating mirrors may be reduced; the swing of the rotating prisms cannot be reduced.

Gated Filter Results

The upper trace of photo 7-1-1 of Figure 16 indicates signal input to the gate. The lower trace indicates output of the gate. Photo 7-1-2 shows ten superimposed traces. No real signal is apparent—only noise appears. The noise generator was then set to zero. The upper trace of photo 7-2-1 was obtained. The function generator real signals appear as downward bulges—one division to the left and one division to the right of center. Other bulges are due to hum. The bright section of the trace (2 cm to right of center) is the gate. Photo 7-2-2 indicates the hum level in the real signal. The hum was not synchronized with the sweep.

Trace A of Figure 17 was obtained by scanning the real signal only. The delay potentiometer has 1000 divisions. The dial was moved five divisions

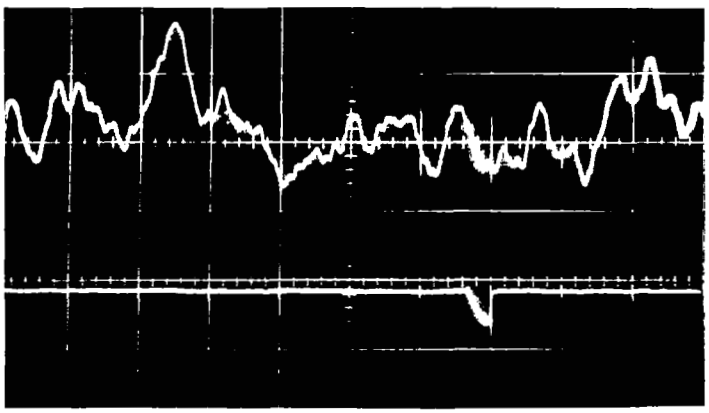

Trace 7-1-1

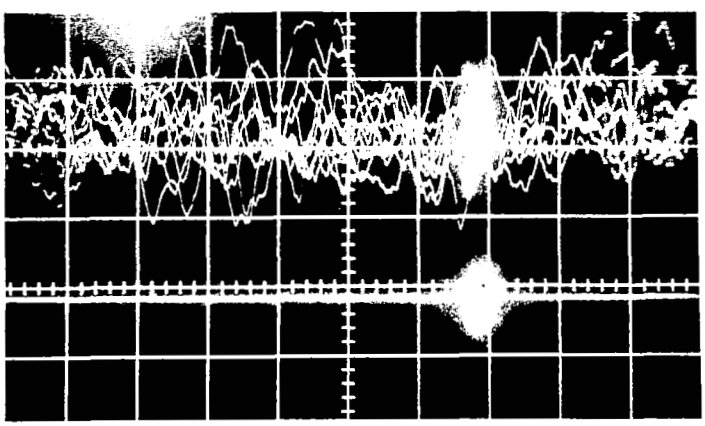

Trace 7-1-2

Figure 16. Gated filter system performance.

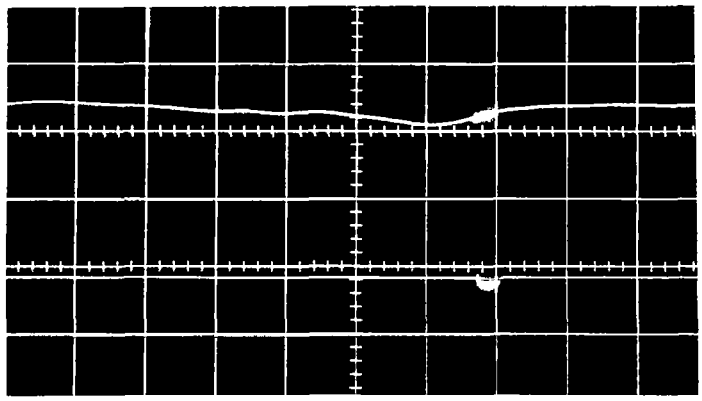

Trace 7-2-1

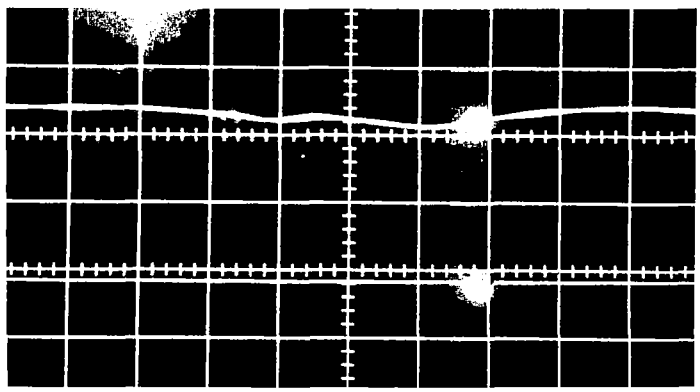

Trace 7-2-2

Figure 16. Gated filter system performance.

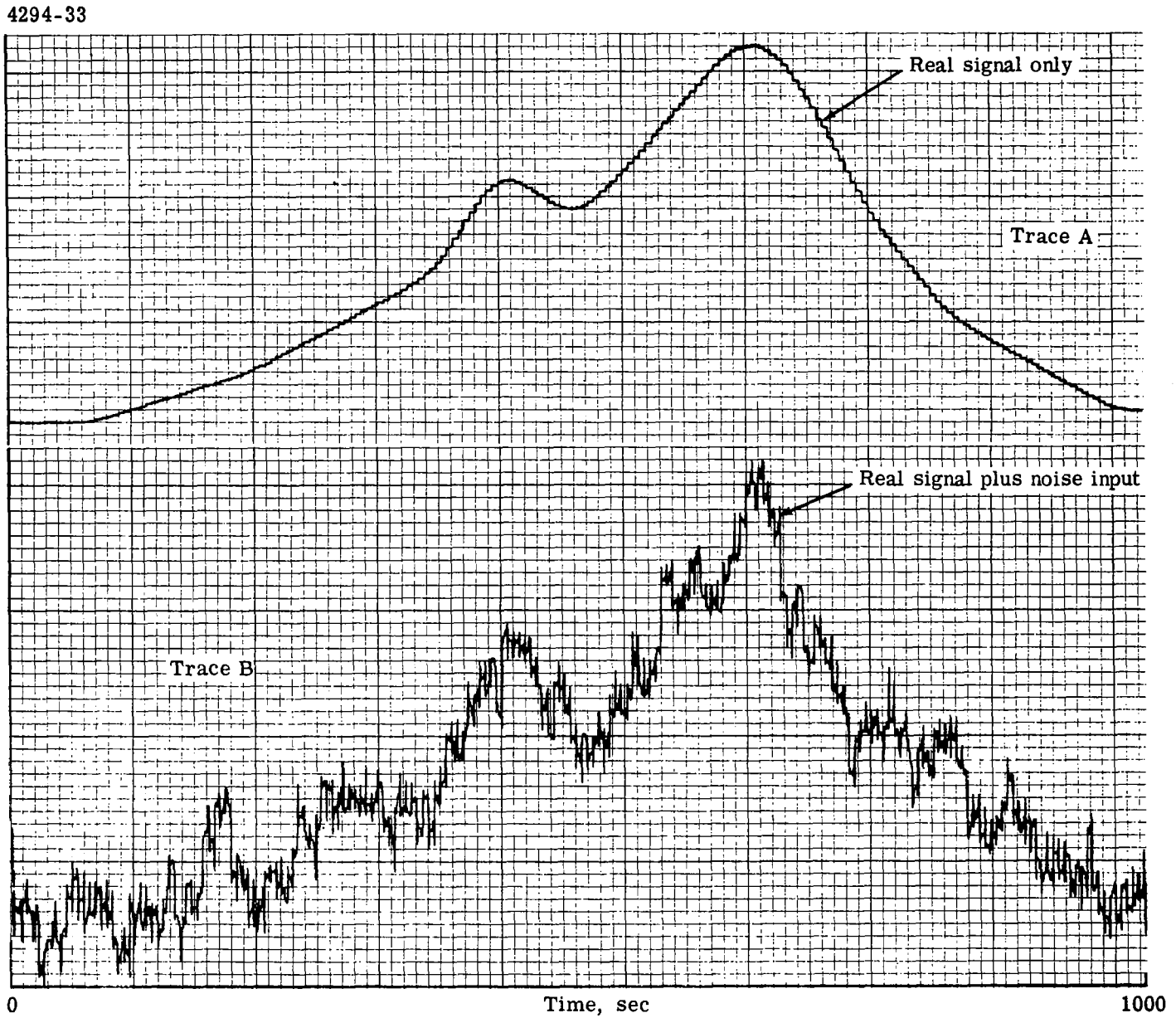

Figure 17. Output curves produced by the gated filter.

every five seconds.* These steps are clearly evident in the trace. The noise generator was then returned to the level indicated in photo 7-1-1 and trace B of Figure 17 was recorded. The real signal was fairly well recovered. The trace may be compared with photo 7-1-2 of Figure 16. The filter time constant was 12 sec. Photo 7-1-1 indicates that more of the high frequency components could have been filtered.

Discussion

In using the gated filter system, care should be exercised in selection of gate width. Noise builds up as the square root of the width. The real signal builds up directly with the width. Conseqently, the real signal will climb out of the noise more quickly as the gate is widened. However, a wide gate eliminates the high frequency components of the real signal. A width approximately one-fifth of the width of the line being sought should be satisfactory.

In a comparison of the digital device and gated filter systems, the following items are significant.

- The gated filter had one storage element; the digital device has 1024.
- The digital device is taking readings all the time; the gated filter reads only during the time that the gate is open.
- The digital device compares its readings with a reference voltage. It records only a "yes" or a "no"—depending on which voltage is the greater. The gated filter records the actual magnitude of the read voltage.

The first two items indicate that the digital device should be superior to the gated filter. The last item indicates an advantage for the gated filter. A system having 1024 analog storage locations would combine the superiorities of both.

---

*A motor drive should be used for extended runs.

Both the digital device and the gated filter permit the photomultiplier output to be scanned at a rate between one and ten sweeps per second. This permits photomultiplier drift to be eliminated. This is a distinct advantage over earlier systems in which a single scan of the spectrum was made and a filter as used to remove the noise.

The digital device is much easier to set up and use. It gives faster results and is capable of revealing signals buried much more deeply in noise. This device is expensive and is a special purpose item.

The gated filter can be assembled from components available in most laboratories. It is adequate for indicating signals for which the signal-to-noise ratio is 0.1 or greater. Drift in the final filter must be eliminated carefully.

Allison Division of General Motors,
Indianapolis, Indiana, 2 July 1965.